Chemical Engineering Journal 143 (2008) 299–307

Contents lists available at ScienceDirect

Chemical Engineering Journal

journal homepage: www.elsevier.com/locate/cej

Synthesis, structural refinement and optical behavior of $CaTiO_3$ powders: A comparative study of processing in different furnaces

L.S. Cavalcante[a,*], V.S. Marques[b], J.C. Sczancoski[a], M.T. Escote[c], M.R. Joya[a], J.A. Varela[d], M.R.M.C. Santos[b], P.S. Pizani[a], E. Longo[d]

[a] LIEC, Universidade Federal de São Carlos, Departamento de Química e Física, P.O. Box 676, 13565-905 São Carlos, SP, Brazil
[b] Centro de Ciências da Natureza, Departamento de Química, Universidade Federal do Piauí, P.O. Box 64049-550, Teresina, PI, Brazil
[c] Centro de Engenharia, Modelagem e Ciências Sociais Aplicadas, Universidade Federal do ABC, Rua Catequese 240, P.O. Box 09090-400, Santo André, SP, Brazil
[d] LIEC-IQ, Universidade Estadual Paulista, P.O. Box 355, 14801-907 Araraquara, SP, Brazil

ARTICLE INFO

Article history:
Received 10 March 2008
Received in revised form 3 May 2008
Accepted 10 May 2008

Keywords:
$CaTiO_3$
Optical materials
Heat treatment
Rietveld refinement
Microwave effects

ABSTRACT

Calcium titanate ($CaTiO_3$) powders were synthesized by the polymeric precursor method and processed in different furnaces. The structural evolution of $CaTiO_3$ powders heat treated in conventional furnace and adapted domestic microwave oven was analyzed by X-ray diffraction (XRD), micro-Raman scattering (MRS) spectroscopy and ultraviolet–visible (UV–vis) absorption spectroscopy. XRD, MRS and Rietveld refinement revealed that the $CaTiO_3$ powders heat treated in both furnaces are free of deleterious phases and crystallize in an orthorhombic structure. UV–vis measurements suggested the presence of intermediary energy levels into the optical band gap of structurally disordered $CaTiO_3$ powders. $CaTiO_3$ powders heat treated in microwave oven showed a rapid structural organization than powders heat treated in conventional furnace. The optical absorption values revealed a different behavior due to the changes in the structural order–disorder degree of the $CaTiO_3$ lattice. The differences verified in the heating process of $CaTiO_3$ powders processed in conventional furnace and adapted domestic microwave oven were discussed.

1. Introduction

Calcium titanate ($CaTiO_3$) was discovered for the first time in mineral form in 1839 by Gustav Rose, a German mineralogist. As ceramic material, $CaTiO_3$ has been widely used in electronic devices and it is a key component of Synroc (type of synthetic rock used to store nuclear waste) [1]. $CaTiO_3$ belongs to the important group of compounds with perovskite-type structure. $CaTiO_3$ exhibits an orthorhombic structure with space group *Pbnm* below 1380 K. The unconventional space group *Pnma* is designed to the "orthorhombic" structure. In temperatures between 1380 and 1500 K occurs a phase transition and changes the space group for *Cmcm*. At 1500 K, the orthorhombic structure transforms to "tetragonal" structure with space group *I*4/*mcm*. Above 1580 K, this material exhibits a "cubic" structure with space group $Pm\bar{3}m$ [2]. Different methods have been reported in the literature for the synthesis of $CaTiO_3$ powders. This perovskite was initially prepared by conventional solid-state reaction between TiO_2 and $CaCO_3$ or CaO at temperatures of approximately 1623 K [3]. However, $CaTiO_3$ powders obtained by this method present several problems, such as high-processing temperatures, inhomogeneity and contamination by impurities with a nonuniform particle sizes distribution [4]. To minimize these problems, wet chemical methods have been employed to synthesize $CaTiO_3$ powders with desired stoichiometry, such as: sol–gel [5], co-precipitation [6], combustion method [7], organic–inorganic solution technique [8] and hydrothermal process [9].

Recently, photoluminescence properties of disordered structurally $CaTiO_3$ have been reported in the literature [10,11]. Moreover, this material can be used for applications in communication systems operated by microwave frequencies (UHF and SHF) [12–14]. In this perovskite, the substitution of the A site (Ca^{2+} ion) by trivalent ions (Sm^{3+} or Nd^{3+}) results in the formation of Ca^{2+} vacancies, which consequently affect the dielectric properties of the material. Generally, the obtained products exhibit high-dielectric constant (ε_r) and low-dielectric loss ($\tan\delta$) [15,16]. These properties suggest a possible application of $CaTiO_3$ as microwave dielectric ceramics, mainly in resonators and filters [17]. Lemanov et al. [18] measured the dielectric properties of $CaTiO_3$ at low temperature and classified this perovskite as an incipient ferroelectric or quantum paraelectric. Wang et al. [19] reported the ferroelectric transition in $CaTiO_3$ using

* Corresponding author. Tel.: +55 16 3361 5215; fax: +55 16 3351 8214.
E-mail address: laeciosc@bol.com.br (L.S. Cavalcante).

1385-8947/$ – see front matter © 2008 Elsevier B.V. All rights reserved.
doi:10.1016/j.cej.2008.05.017

the first-principles calculation and considering the Ti atom displaced in the [0 0 1] direction. The obtained results for these authors revealed that the $CaTiO_3$ presents an incipient ferroelectric behavior. The literature also reports the substitution of the Ca^{2+} ions by Pr^{3+} and Er^{3+} ions, which are able to improve of optical performance in $CaTiO_3$, such as red emission phosphors, strong green up conversion luminescence and blue emission [20–24].

In order to obtain well-crystallized $CaTiO_3$ powders by the polymeric precursor method is necessary high-heat treatment temperatures for long times (≥120 min) [25]. Therefore, a possible alternative to decrease this factor can be the use of microwave energy. Currently, the microwave energy has received considerable attention due to their interesting advantages, such as: reduced processing costs, better production quality and possibility of formation of new materials or products, among others. In this case, several technologically important materials can be heated rapidly, uniformly, selectively, less expensively and with high control than the conventional methods [26].

$CaTiO_3$ powders present interesting photoluminescence (PL) properties at room temperature. This optical property is dependent on the structural organization level, preparation method and heat treatment conditions [27]. Therefore, it is important to understand the influence of different processing methods on the structural organization degree and optical properties of this material.

In this paper, we report the synthesis of $CaTiO_3$ powders prepared by the polymeric precursor method and heat treated at different temperatures in an adapted domestic microwave oven for 30 min and conventional furnace for 120 min. The obtained powders were characterized by X-ray diffraction, micro-Raman scattering, Rietveld refinement and ultraviolet–visible absorption spectroscopy. Moreover, we show the differences between the heating process of $CaTiO_3$ powders by microwave radiation in microwave oven (MO) and thermal radiation in conventional furnace (CF).

2. Experimental details

2.1. Synthesis of $CaTiO_3$ powders

$CaTiO_3$ powders were synthesized by the polymeric precursor method [28]. Calcium carbonate, $CaCO_3$ (99.9% purity Aldrich), titanium (IV) isopropoxide [$Ti(OC_3H_7)_4$] (99.9% purity Aldrich), ethylene glycol, $C_2H_6O_2$ (99% purity J.T. Baker) and citric acid anhydrous, $C_6H_8O_7$ (99.5% purity Synth) were used as starting materials. [$Ti(OC_3H_7)_4$] was quickly added in $C_6H_8O_7$ aqueous solution to avoid hydrolysis reaction of the alkoxide with air environment. Clear and homogenous titanium citrate was formed under constant stirring at 353 K for several hours. In the following step, the gravimetric procedure was realized for the correction and determination of the stoichiometric value correspondent to the TiO_2 mass (g) into the titanium citrate. $CaCO_3$ was dissolved and added in a stoichiometric quantity into the Ti citrate. After solution homogenization containing Ca^{2+} cations, $C_2H_6O_2$ was added to promote citrate polymerization by the polyesterification reaction [29]. The citric acid/ethylene glycol mass ratio was fixed at 60:40. The solution was slowly heated at 373 K under constant stirring to allow the evaporation of water and formation of the polymeric resin. The obtained polymeric resin was then placed in a conventional furnace and heated treated at 623 K for 240 min, promoting the pulverization of the polymeric resin and formation of the precursor powders. Finally, these disordered powders were heat treated at different temperatures for 120 min with a heating rate of 274 K/min in a CF and for 30 min with a heating rate of 298 K/min in an adapted domestic MO [30].

2.2. Characterizations of $CaTiO_3$ powders

In these experiments, the powders heat treated at different temperatures in CF and MO were characterized by X-ray diffraction (XRD) recorded on a Rigaku-DMax2500PC (Japan) with Cu Kα radiation in the 2θ range from 5° to 75° with 0.02°/min. Rietveld analyses were performed in a step scan mode in the 2θ range from 17° to 110°, angular step of 0.02° and exposure time of 2 s. Micro-Raman scattering (MRS) measurements were recorded using a T-64000 Jobin-Yvon (France) triple monochromator coupled to a CCD detector. The spectra were obtained using a 514.5 nm line of an argon ion laser, keeping their maximum output power at 9 mW. A 100 μm lens was used to prevent overheating of the powders. Ultraviolet–visible (UV–vis) spectroscopies for the spectral dependence of optical absorbance for the $CaTiO_3$ powders were taken using a Cary 5G (Varian, USA) equipment in total reflection mode. All measurements were performed at room temperature.

3. Results and discussion

3.1. X-ray diffraction analyses

Fig. 1a and b show the XRD patterns of $CaTiO_3$ powders heat treated at different temperatures for 30 min in MO and 120 min in CF under air atmosphere, respectively.

The presence of diffraction peaks can be used to evaluate the structural order at long range or periodicity of the material. $CaTiO_3$ phase was confirmed by the comparison between the XRD patterns with the respective Inorganic Crystal Structure Database (ICDS) no. 06-2149 [31]. All diffraction peaks can be assigned to the orthorhombic structure. $CaTiO_3$ powders heat treated at several temperatures for 30 min in MO exhibited characteristic diffraction peaks correspondent to an ordered structure at long range (Fig. 1a). However, no diffraction peaks were verified for the $CaTiO_3$ powders heat treated at 673, 723 and 773 K for 120 min in CF. This behavior is typical of amorphous or disordered materials (Fig. 1b). The lattice parameters analyses were performed to verify the differences on the structural organization degree at long range. The experimental lattice parameters were calculated using the least square refinement from the UNITCELL-97 program [32].

Table 1 shows the lattice parameters values for the $CaTiO_3$ powders heat treated at different temperatures for 30 min in MO and 120 min in CF under air atmosphere.

The good agreement between the experimental lattice parameters values with the respective ICSD card shows that the heat treatment evolution leads to an increase of crystallinity on the $CaTiO_3$ powders (Table 1). All diffraction peaks were identified as belonging to the $CaTiO_3$ phase in agreement with the ICSD no. 06-2149. Fig. 2a and b show the lattice parameters evolution (*a*, *b* and *c*) of $CaTiO_3$ powders as a function of temperature in both the furnaces.

As can be seen in these figures, the lattice parameters of $CaTiO_3$ powders with orthorhombic structure present small deviations as indicated by the error bars. The increase of temperature leads to the formation of $CaTiO_3$ phase in both the furnaces. Also, it was observed in the range from 923 to 973 K a significant change in the *c* lattice parameter value, which probably can be associated with the presence of defects due to the structural disorder in the $CaTiO_3$ lattice. In addition, we observed small deviations in the lattice parameters for the $CaTiO_3$ powders heat treated in CF. A better estimative of the lattice parameters was performed by Rietveld

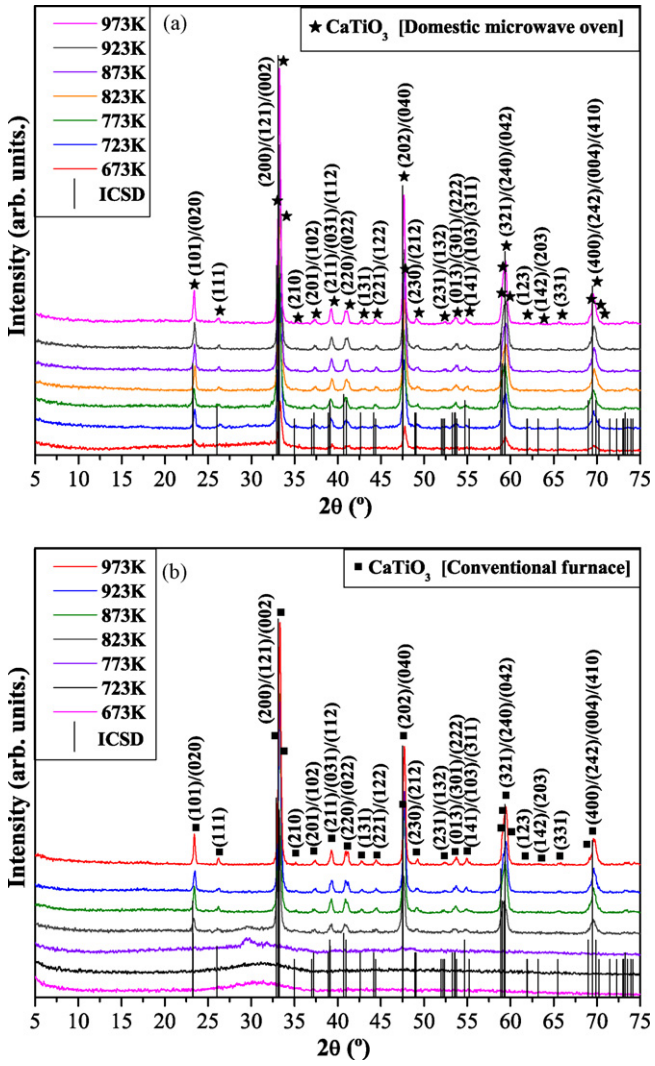

Fig. 1. XRD patterns of $CaTiO_3$ powders heat treated at different temperatures for (a) 30 min in MO and (b) 120 min in CF, both under air atmosphere.

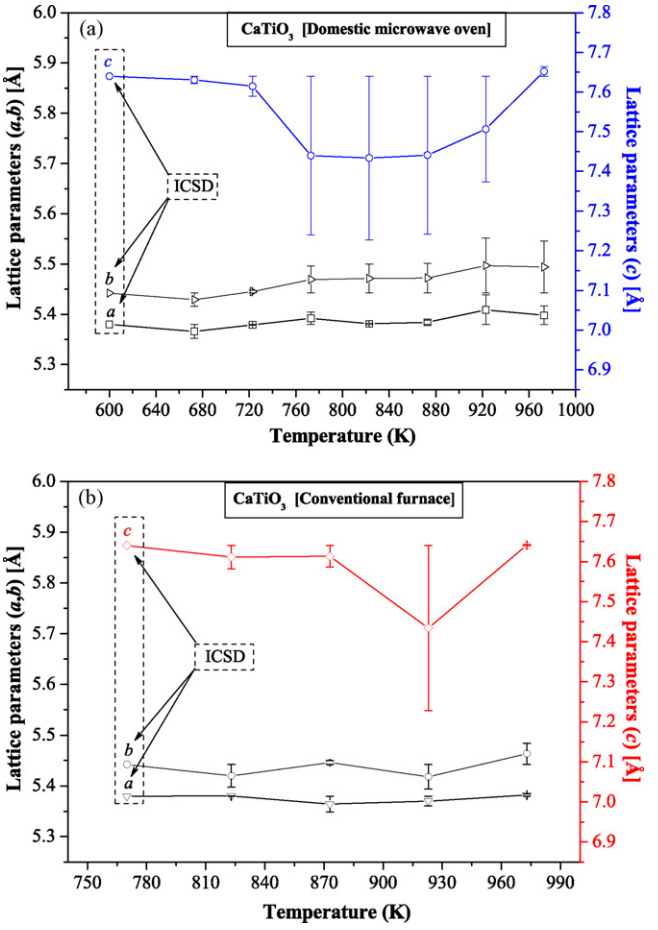

Fig. 2. *a*, *b* and *c* lattice parameters as a function of temperature for the $CaTiO_3$ powders processed in different furnaces: (a) MO for 30 min and (b) CF for 120 min. The vertical bars show the standard mean error.

refinement for the $CaTiO_3$ powders heat treated at 973 K for 30 min in MO and 120 min in CF.

The average crystallite sizes were estimated by the Scherrer's equation using the full width at half maximum (FWHM) of the most intense peak (1 2 1). As reported in the literature [33], the Scherrer's equation (Eq. (1)) is described as follows:

$$D = \frac{0.9\lambda}{B\cos\theta} \quad (1)$$

where D is the average crystallite size or particle size, λ the X-ray wavelength (0.1540593 nm), θ the Bragg angle and B is the FWHM.

Fig. 3a and b shows the obtained results for the average crystallite sizes of $CaTiO_3$ powders heat treated at different temperatures for 30 min in MO and 120 min in CF under air atmosphere. These data are listed in Table 1.

As can be seen, the increase of temperature promotes an increase in the average crystallite size or particle size. This behavior can be associated with the aggregates production and nuclei formation [34].

Table 1
Data obtained by XRD analyses of $CaTiO_3$ powders heat treated in different furnaces

Temperature (K)	Time (min)	*a* lattice parameter (Å)	*b* lattice parameter (Å)	*c* lattice parameter (Å)	Particle size (nm)
673	30	5.366(8)	5.429(4)	7.631(9)	21.22
723	30	5.379(6)	5.445(6)	7.615(2)	22.37
773	30	5.392(8)	5.469(1)	7.440(4)	22.42
823	30	5.382(5)	5.471(8)	7.434(2)	23.06
873	30	5.384(3)	5.472(8)	7.441(2)	23.61
923	30	5.409(8)	5.497(1)	7.507(1)	25.51
973	30	5.398(9)	5.494(5)	7.652(5)	27.30
873	120	5.380(3)	5.420(8)	7.611(6)	23.48
823	120	5.364(2)	5.446(4)	7.613(9)	25.37
923	120	5.370(4)	5.418(8)	7.434(4)	26.06
973	120	5.382(9)	5.463(4)	7.641(1)	28.11
ICSD no. 06-2149		5.3796(1)	5.4423(3)	7.6401(5)	–

3.2. Rietveld refinement analyses

Fig. 4a and b shows the Rietveld analyses [35] of crystalline $CaTiO_3$ powders heat treated at 973 K for 30 min in MO and 2 h in CF under air atmosphere, respectively.

These analyses were performed with the FULLPROF program [36], assuming *Pbnm* space group for an orthorhombic distorted perovskite-type structure. We utilize the pseudo-Voigt function as described by Finger et al. [37], in order to fit the several parameters to the data point: one scale factor, one zero shifting, four background, three cell parameters, five shape and width of the peaks, one global thermal factor and two asymmetric factors. A typical example of these analyses is shown in Fig. 4a and b, which present the experimental and calculated XRD patterns obtained by the refinements of $CaTiO_3$ phase. The strain anisotropy broadening was corrected by the phenomenological model described by Stephens [38]. Fig. 4 shows the good agreement between the calculated and observed X-ray patterns for the $CaTiO_3$ powders heat treated at 973 K for 30 min in MO and 973 K for 120 min in CF. The good agreement between the refined crystallographic data and structural parameters are listed in Table 2.

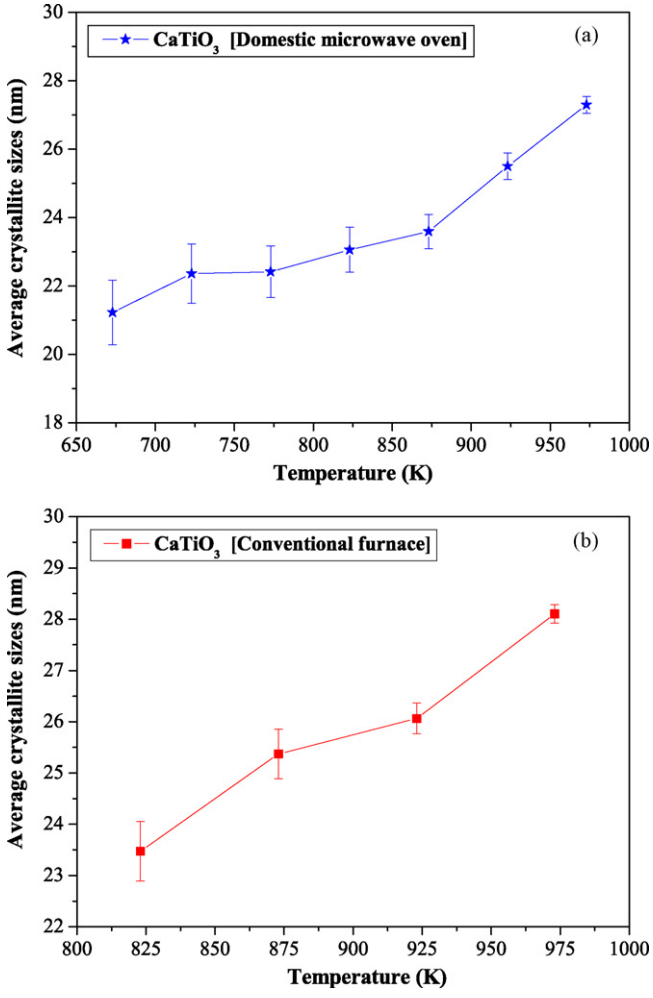

Fig. 3. Average crystallite sizes as a function of heat treatment of $CaTiO_3$ powders: (a) 30 min in MO and (b) 120 min in CF. The vertical bars show the standard mean error.

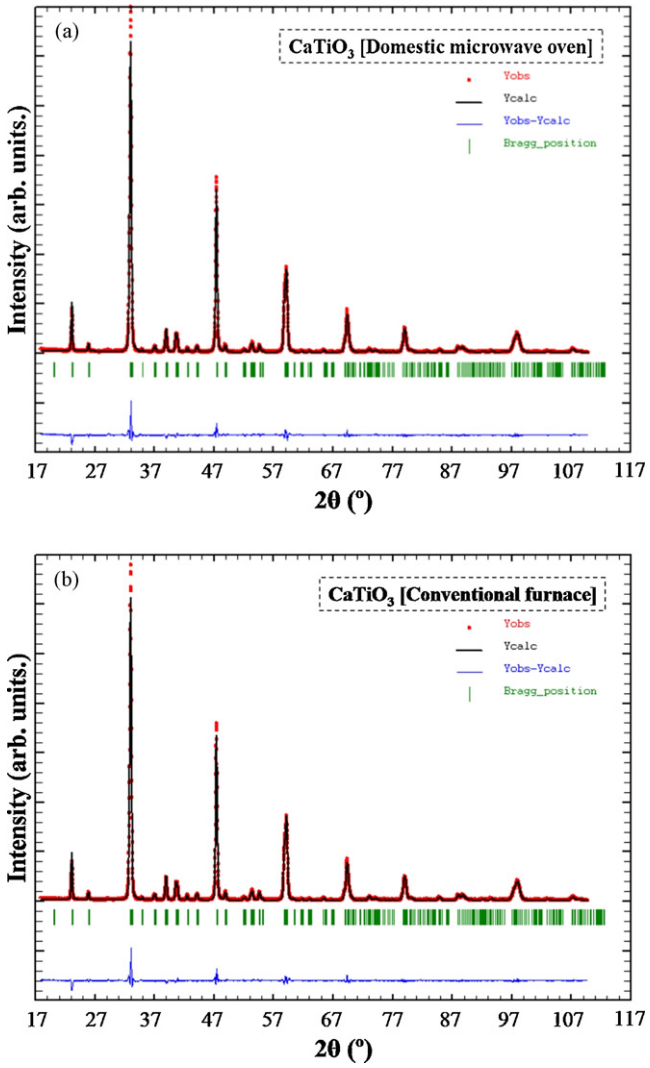

Fig. 4. Rietveld analyses for crystalline $CaTiO_3$ powders heat treated at 973 K for 30 min in (a) MO and for 120 min in (b) CF, both under air atmosphere.

3.3. Micro-Raman scattering analyses

Fig. 5a and b show the MR spectra of $CaTiO_3$ powders heat treated at different temperatures for 30 min in MO and 120 min in CF under air atmosphere, respectively.

The structural order–disorder degree at short range was evaluated by micro-Raman scattering spectroscopy. There are 24 Raman-active modes for orthorhombic structure with space group *Pbnm* ($Z^B = 4$) with four molecular units in the primitive cell, which can be described by the representation $\Gamma_{Raman,Pbnm} = 7A_g + 5B_{1g} + 7B_{2g} + 5B_{3g}$. The nine Raman modes observed in the range from 145 to 815 cm^{-1} are attributed to the orthorhombic structure, in agreement with the literature [39–45]. Table 3 presents the positions of nine Raman modes (P_1–P_9) for the $CaTiO_3$ powders heat treated at 973 K for 30 min in (a) MO and 120 min in (b) CF. In this table also are shown a comparative between the Raman modes obtained in this work with those reported in the literature by different methods. P_1 Raman mode is related to the $CaTiO_3$ lattice mode. P_2, P_3, P_4, P_5 and P_6 are attributed to the O–Ti–O bending modes. P_7 and P_8 are ascribed to the torsional mode and P_9 is assigned to the Ti–O symmetric stretching vibration. All $CaTiO_3$ powders heat treated at different temperatures for 30 min with microwave radiation exhibited a

Table 2
Lattice parameters, *R*-factors and positional parameters obtained from the Rietveld analyses of $CaTiO_3$ powders heat treated in different furnaces (ICDS no. 06-2149)

Refined parameters	Units	Results
Temperature, 973 K; time, 30 min; microwave oven[a]		
a	Å	5.3914(0)
b	Å	5.4425(4)
c	Å	7.6526(4)
x_{Ca}	–	0.0053
y_{Ca}	–	0.03283
z_{Ca}	–	0.25
B_{Ca}	–	0.2089
$F_{(occup)Ca}$	–	0.5
x_{Ti}	–	0
y_{Ti}	–	0.5
z_{Ti}	–	0
B_{Ti}	–	0.2089
$F_{(occup)Ti}$	–	0.5
x_{O1}	–	0.58805
y_{O1}	–	−0.01377
z_{O1}	–	0.25
B_{O1}	–	0.2089
$F_{(occup)O1}$	–	0.5
x_{O2}	–	0.28822
y_{O2}	–	0.28826
z_{O2}	–	0.03134
B_{O2}	–	0.2089
$F_{(occup)O2}$	–	1
Temperature, 973 K; time, 120 min; conventional furnace[b]		
c	Å	5.3924(7)
a	Å	5.4454(3)
b	Å	7.6548(8)
x_{Ca}	–	0.00641
y_{Ca}	–	0.03378
z_{Ca}	–	0.25
B_{Ca}	–	0.16514
$F_{(occup)Ca}$	–	0.5
x_{Ti}	–	0
y_{Ti}	–	0.5
z_{Ti}	–	0
B_{Ti}	–	0.16514
$F_{(occup)Ti}$	–	0.5
x_{O1}	–	0.58399
y_{O1}	–	−0.01492
z_{O1}	–	0.25
B_{O1}	–	0.16514
$F_{(occup)O1}$	–	0.5
x_{O2}	–	0.28855
y_{O2}	–	0.28920
z_{O2}	–	0.03369
B_{O2}	–	0.16514
$F_{(occup)O2}$	–	1

[a] R_{Bragg} = 4.601, R_p = 6.95, R_{wp} = 9.41, R_{exp} = 5.25 and χ^2 = 3.21 (MO).
[b] R_{Bragg} = 4.120, R_p = 8.15, R_{wp} = 10.5, R_{exp} = 6.29, χ^2 = 2.80 (CF).

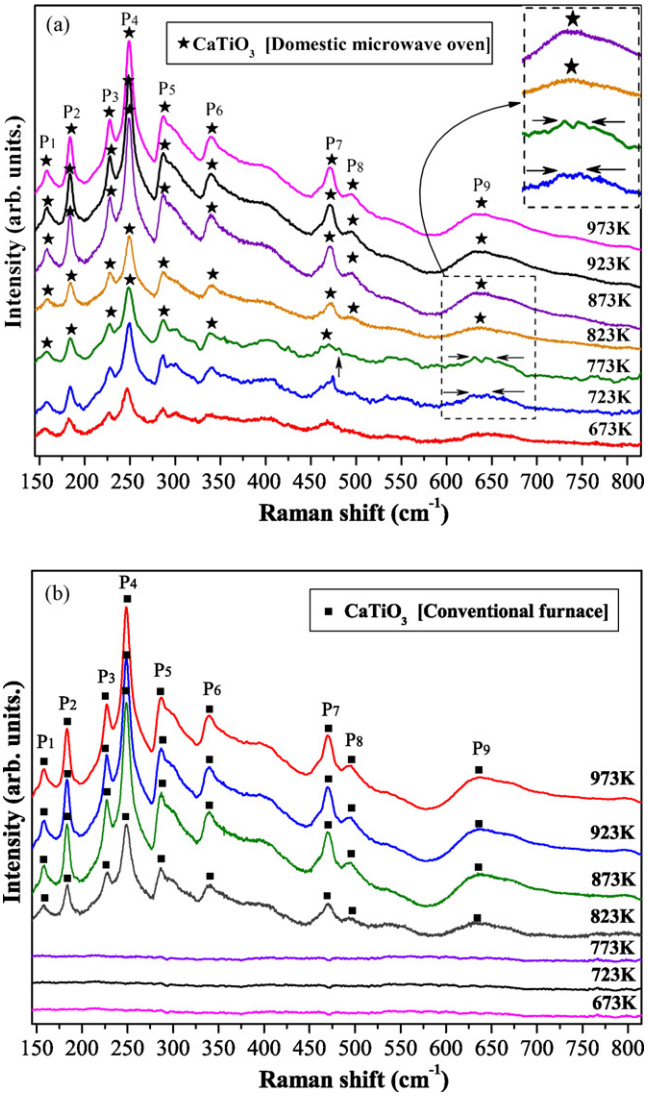

Fig. 5. MRS spectra of $CaTiO_3$ powders heat treated at different temperatures for 30 min in (a) MO and 120 min in (b) CF, both under air atmosphere. The zoom in Fig. 5(a) shows the 600–700 cm^{-1} region.

high-structural organization degree, as can be seen in MRS spectra (Fig. 5a).

However, some Raman modes are not well defined for the $CaTiO_3$ powders heat treated at 673, 723 and 773 K. The vertical arrow indicates the presence of a peak at 494.5 cm^{-1}, which is assigned to the Ti–O torsional (bending or internal vibration of the oxygen cage) mode. This result is similar to the reported by Balachandran and Eror [39]. The two horizontal arrows presented in

Table 3
Data obtained by MRS spectra analyses of $CaTiO_3$ powders heat treated in different furnaces in comparison with other methods reported in the literature

Method	Temperature (K)	Time (min)	P_1	P_2	P_3	P_4	P_5	P_6	P_7	P_8	P_9	Reference
LMT	1073	–	155	180	226	247	286	337	471	495	–	[39]
SSR	1873	2880	153	178	222	244	281	333	467	490	–	[40]
–	–	–	154	181	225	246	284	300	469	493	–	[41]
SSR	1323	4320	154	181	225	246	286	335	470	494	–	[42]
SSR	1523	1080	–	175	224	244	286	336	471	492	677	[43]
SSR	1923	240	–	183	227	247	288	339	470	494	641	[44]
–	–	–	155	181	226	248	290	340	470	496	–	[45]
PPM	973	30	158	184	228	249	287	340	471	497	637	This work
PPM	973	120	157	183	227	248	287	339	470	496	640	This work

LMT = liquid mix technique; SSR = solid-state reaction; PPM = polymeric precursor method; P_n = peak number (cm^{-1}).

Table 4
Data obtained by UV–vis spectra for $CaTiO_3$ powders heat treated in different furnaces in comparison with others methods reported in the literature

Method	Temperature (K)	Time (min)	Optical band gap (eV)	Reference
CPP	873	300	3.55	[48]
HT	770	–	3.5	[49]
PPM	873	120	3.48	[50]
CSS	1673	720	3.3	[51]
–	–	–	3.70	[52]
PPM	673	30	2.58	This work
PPM	723	30	3.29	This work
PPM	773	30	3.32	This work
PPM	823	30	3.34	This work
PPM	873	30	3.35	This work
PPM	923	30	3.38	This work
PPM	973	30	3.41	This work
PPM	773	120	2.82	This work
PPM	823	120	3.35	This work
PPM	873	120	3.37	This work
PPM	923	120	3.39	This work
PPM	973	120	3.42	This work

CPP = complex polymer precursor; HT = hydrothermal; PPM = polymeric precursor method; CSS = conventional solid state.

the inset zoom of Fig. 5a show two small peaks, suggesting the simultaneous presence of $[TiO_6]$ and $[TiO_5]$ clusters, which can be observed by X-ray absorption near-edge structure [46]. The incomplete organization of the $CaTiO_3$ lattice can be attributed to the defects in the covalent bond due to the oxygen vacancies ($V_O^{\bullet\bullet}$) between the clusters $[TiO_6–TiO_5{\cdot}V_O^{\bullet\bullet}]$. The formation of Ti–O bond was observed after heat treatment at 823 K for 30 min, when the $CaTiO_3$ lattice is more ordered. The peak localized at 641 cm^{-1} is assigned to the Ti–O symmetric stretching vibration, suggesting the presence of a system more organized when heat treated from 873 to 973 K for 120 min in FC and 30 min in MO. The Raman-active modes were not detected for the $CaTiO_3$ powders heat treated at 673, 723 and 773 K for 120 min in CF, evidencing a disordered structure behavior. However, Raman-active modes were only observed for the $CaTiO_3$ powders heat treated from 873 to 973 K for 120 min, confirming the structural order at short range (Fig. 5b).

3.4. Ultraviolet–visible absorption spectroscopy analyses

Fig. 6 shows the UV–vis spectra for the $CaTiO_3$ powders heat treated at different temperatures for 30 min in MO and 120 min in CF under air atmosphere. The optical band gap values obtained through the linear fitting of tails from the UV–vis spectra are shown in Fig. 6a–d and listed in Table 4.

The exponential optical absorption edge and optical band gap are controlled by the structural order–disorder degree in the $CaTiO_3$ lattice. According to Wood and Tauc [47], the optical band gap energy is related to the absorbance and photon energy by Eq. (2):

$$h\nu\alpha \propto (h\nu - E_g^{opt})^2 \quad (2)$$

where α is the absorbance, h the Planck constant, ν the frequency, and E_g^{opt} is the optical band gap energy.

The increase of optical band gap value can be ascribed to the reduction of defects or impurities that give rise to the intermediary energy levels into the band gap of disordered $CaTiO_3$ powders. The $CaTiO_3$ powders heat treated from 673 to 773 K for 30 min in MO and 773 K for 120 min presented a similar spectral dependence behavior as observed in disordered or amorphous semiconductors, such as silicon and insulators (Fig. 6a and d). However, this disorder degree can be reduced by the increase of heat treatment temperature in both processing methods (MO and CF). $CaTiO_3$ powders heat treated from 823 to 873 K for 30 min in MO and 120 min in CF (Fig. 6c–e) revealed a structural order–disorder in the lattice, which can be associated with the presence of defects into the band gap. In addition, $CaTiO_3$ powders heat treated from 923 to 973 K presented typical band gap values of ordered or crystalline materials. The high-optical band gap values for $CaTiO_3$ powders can be observed in the absorbance curves presented in Fig. 6c and e and inset Fig. 6e. As can be seen in Fig. 6f, the progressive heat treatment promotes a reduction on the structural disorder and increase the inclination angle of the dashed line or tail, decreasing the deviations verified by the error bars.

It was observed that the optical absorption measurements were extremely sensitive to the changes in the lattice or variations on the structural order–disorder degree. Table 4 shows a comparative between the optical band gap values of $CaTiO_3$ obtained in this work with those reported in the literature by different methods. As can be seen in this table, the optical band gap is dependent of the preparation method and structural order degree of the lattice [48–52]. In disordered $CaTiO_3$ powders processed in MO and CF, the absorbance measurements suggest a nonuniform band gap with a tail of localized states between the valence band and conduction band. Our results show that the defects in the lattice of $CaTiO_3$ powders processed in low temperatures (623, 723 and 773 K) can be responsible by the differences between the optical band gap values.

3.5. $CaTiO_3$ powders processed in domestic microwave oven and conventional furnace

$CaTiO_3$ powders heat treated at 673, 723 and 773 K for 30 min in MO showed a rapid structural organization than the powders heat treated under the same temperature conditions for 120 min in CF. It was observed a different optical absorption behavior on the $CaTiO_3$ powders processed by microwave radiation. Fig. 7 shows a simple schematic representation of the heating process by domestic microwave oven and conventional furnace.

Fig. 7(a) presents a digital photo of an adapted domestic microwave oven used in the processing of $CaTiO_3$ powders at different temperatures for 30 min. In the interior part of this equipment, the processing of $CaTiO_3$ powders occurs by means of microwave radiation. These powders were placed within an alumina crucible with thick walls and high density to prevent overheating and contamination of the samples. This crucible was positioned on a silicon carbide (SiC) tablet fixed on an alumina refractory in the interior part of the adapted domestic microwave oven. The thick walls of the crucible were able to reduce drastically the heat transferred by thermal conduction from the SiC for the powders. The temperature of $CaTiO_3$ powders was measured through a thermocouple coated with alumina. This thermocouple was placed in direct contact with these powders to ensure the reliability of the measurements. More details in ref [30] on the adapted domestic microwave oven employed in this work. The obtained results by XRD, MRS and UV–vis confirm that the $CaTiO_3$ powders processed in MO presents a rapid structural organization compare to the processed in CF. This behavior can be related with the heating process in MO, which occurs from the interior to the surface for the $CaTiO_3$ powders (Fig. 7(b) and (c)). The microwave energy is transformed in heat through the interaction between molecules and atoms with the electromagnetic field. This interaction results in an internal and volumetric heating of the powders, promoting the formation of temperature gradients and heat flows [53]. In particular, the chemical method employed for the synthesis of $CaTiO_3$ powders presents residual organic compounds arising from the citric acid and ethylene glycol. These organic compounds when pulverized generate amorphous carbon powders, which are able to absorb rapidly the microwaves (2.45 GHz frequency) and consequently to increase the temperature at approximately 1556 K in just 1 min in a MO system operating at 1 kW [54]. Therefore, we believe that this behavior can

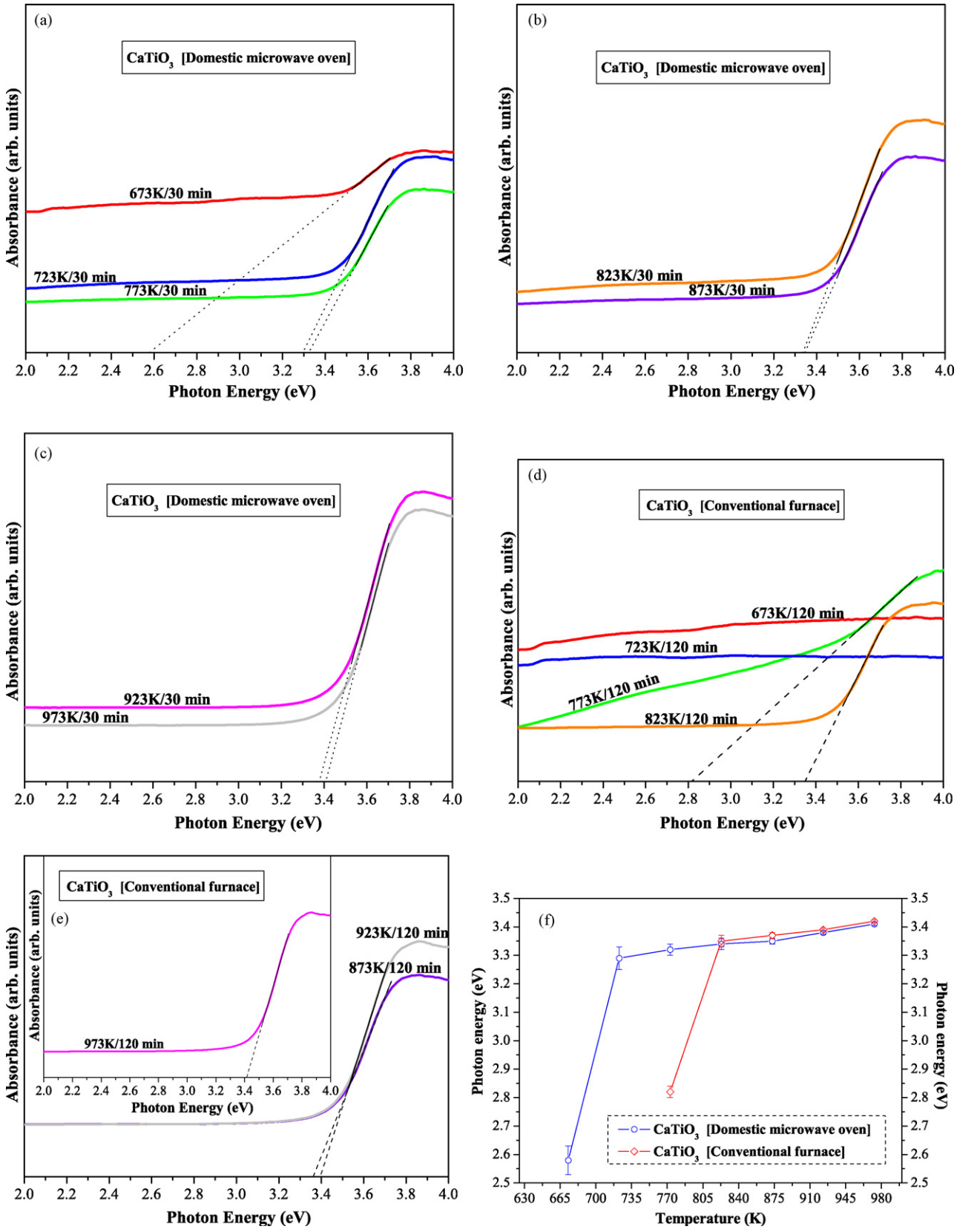

Fig. 6. UV–vis absorbance spectra for the $CaTiO_3$ powders heat treated in the range from (a) 673 to 773 K for 30 min in MO, (b) 823–873 K in MO, (c) 923–973 K, (d) 673–823 K for 120 min and (e) 873–973 K for 120 min under air atmosphere. Inset shown in Fig. 6(e) shows the $CaTiO_3$ powders heat treated at 973 K for 120 min in CF under air atmosphere. The dashed lines correspond to the respective tails. (f) Optical band gap evolution with the increase of temperature for $CaTiO_3$ processed in different furnaces (MO and CF). The vertical bars show the standard mean error.

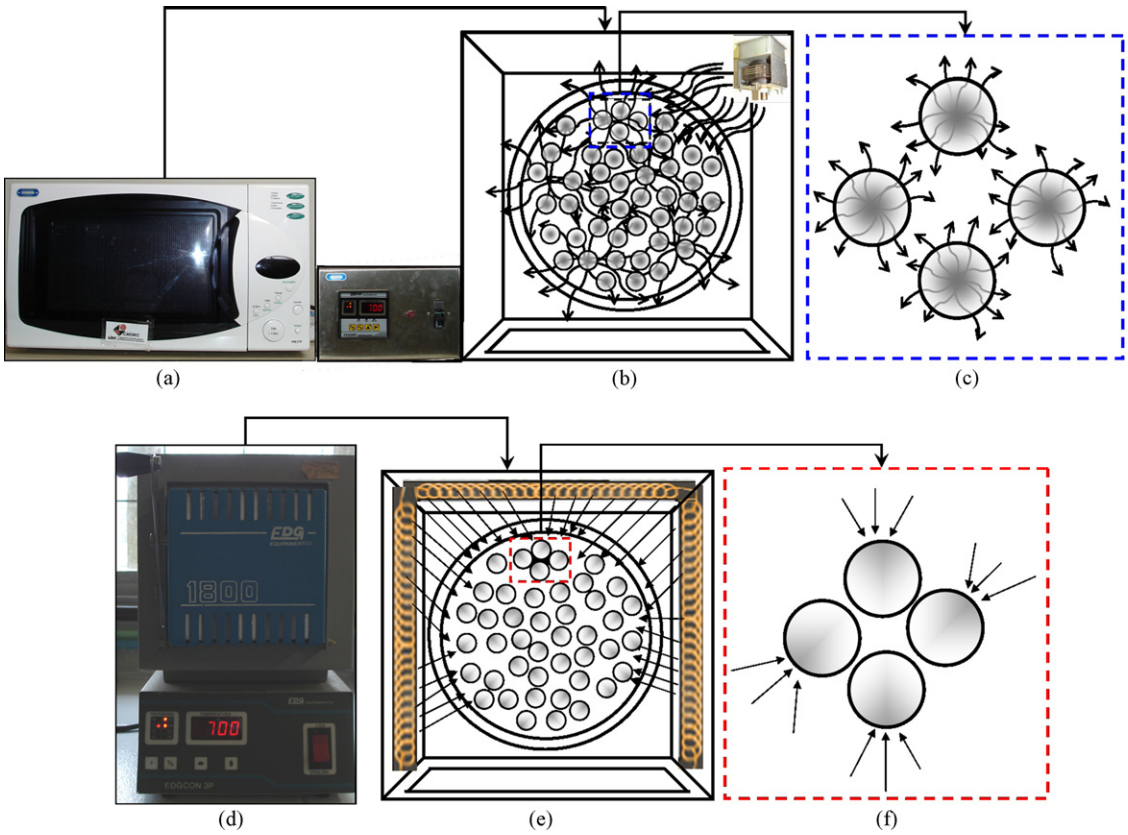

Fig. 7. (a) Adapted domestic microwave oven for processing of $CaTiO_3$ powders. (b) Interior of microwave oven: magnetron, $CaTiO_3$ powders, susceptor of SiC and refractory. (c) Direction and interaction of the heat flow in the heating of $CaTiO_3$ powders in MO. (d) Commercial conventional furnace. (e) Interior of conventional furnace: electric resistances, $CaTiO_3$ powders, refractory. (f) Direction and interaction of the heat flow in the heating of $CaTiO_3$ powders in CF.

significantly contribute with a rapid formation kinetic of $CaTiO_3$ phase. In addition, MO system employed in this work was operated with a maximum power of 900 W. According to the literature [55], the rapid phase formation can also be related with the TiO_2, which is able to absorb partially the microwave radiation. In contrast, CaO shows a poor coupling with the microwave radiation, i.e., this oxide is considered a semitransparent material for this energy type. In general, few materials are completely transparent or absorbent of microwave energy [56]. Our obtained results can also be explained by the formation of carbon monoxide (gaseous product) during the processing, which could provide a reductive atmosphere around of the sample. In this case, Ti^{4+} is partially reduced to Ti^{3+}, resulting in a strong interaction with the microwaves [57,58]. As can be seen in Fig. 7(c), the heat flow in the heating process occurs in large part on the interior of the powders than on the surface. This mechanism probably can be responsible by the rapid heating of $CaTiO_3$ powders. Recently, the literature reported the crystallization of $CaBi_4Ti_4O_{15}$ thin films by a domestic microwave oven for 973 K at few minutes [59].

Fig. 7(d) illustrates a digital photo of a commercial conventional furnace used in the processing of $CaTiO_3$ powders at different temperatures for 120 min. This processing occurs in the interior part of the furnace through the thermal energy. In this case, the electrical resistances provide the thermal energy transferred to the powders (Fig. 7(e)). Fig. 7(f) shows the heating process of $CaTiO_3$ powders by CF. Heating process in CF begins from the surface to the interior of $CaTiO_3$ powders. The characterizations performed by XRD, MRS and UV–vis showed that the $CaTiO_3$ powders processed at 673, 723 and 773 K for 120 min exhibit a structural disorder. Possibly, this behavior is associated to the transference of heat by thermal radiation, heating mainly the surface of the material. In this case, the $CaTiO_3$ lattice no presents a complete internal organization. When occurs the increase of processing time and heat treatment temperature, the thermal energy is transferred to the interior of the material, which contributes significantly for the structural organization of the $CaTiO_3$ lattice.

4. Conclusions

$CaTiO_3$ powders prepared by the polymeric precursor method were processed in CF and MO. XRD, Rietveld refinement and MRS analyses confirmed that $CaTiO_3$ powders processed in both furnaces are free of deleterious phases. Small variations in the lattice parameters were observed on the crystalline $CaTiO_3$ powders processed in CF and MO heat treated at 973 K. Rietveld analyses confirmed that the powders crystallize in an orthorhombic structure with space group *Pbmn* at room temperature. XRD results suggested that the crystallization process of $CaTiO_3$ powders processed in CF begins at 823 K while in MO occurs at 823 K. MRS analyses revealed that $CaTiO_3$ powders heat treated in the range from 673 to 773 K exhibit a structural disorder at short range. However, these powders processed in MO under the same temperature conditions revealed a structural order–disorder. UV–vis spectra indicated the presence of localized energy levels into the optical band gap of disordered $CaTiO_3$ powders processed in CF and MO. These energy levels decrease when occurs an increase of structural order degree in the lattice. The structural evolution of $CaTiO_3$ powders processed in CF and MO was observed through the optical band gap values, which are sensitive to the changes in the lattice. Finally, the use of microwave energy in the processing of $CaTiO_3$ powders prepared by the polymeric precursor method is able to promote a rapid structural organization of the lattice. The

processing of $CaTiO_3$ powders by MO presented many advantages compare to the CF, including the high-reaction kinetics and rapid structural organization at low temperatures (673, 723 and 773 K). XRD patterns, Rietveld, MRS and UV–vis measurements revealed that $CaTiO_3$ powders heat treated at 973 K for 120 min in CF present a high-structural order degree.

Acknowledgements

The authors thank the financial support of the Brazilian research financing institutions: CAPES, CNPq and FAPESP.

References

[1] A.E. Ringwood, S.E. Kesson, K.D. Reeve, D.M. Levins, E.J. Ramm, in: W. Lutze, R.C. Ewing (Eds.), Radioactive Waste Forms for the Future, Elsevier, Amsterdam, 1988, p. 233.
[2] B.J. Kenndey, C.J. Howard, B.C. Chakoumakos, Phase transitions in perovskite at elevated temperatures—a powder neutron diffraction study, J. Phys.: Conden. Matter 11 (1999) 1479–1488.
[3] H.F. Kay, P.C. Bailey, Structure and properties of $CaTiO_3$, Acta Cryst. 10 (1957) 219–226.
[4] I.R. Evans, J.A.K. Howard, T. Sreckovic, M.M. Ristic, Variable temperature in situ X-ray diffraction study of mechanically activated synthesis of calcium titanate, $CaTiO_3$, Mater. Res. Bull. 38 (2003) 1203–1213.
[5] G. Pfaff, Synthesis of calcium titanate powders by the sol–gel process, Chem. Mater. 6 (1994) 58–62.
[6] X. Zhang, J. Zhang, X. Ren, X.-J. Wang, The dependence of persistent phosphorescence on annealing temperatures in $CaTiO_3$:Pr^{3+} nanoparticles prepared by a coprecipitation technique, J. Solid State Chem. 181 (2008) 393–398.
[7] M. Muthuraman, K.C. Patil, S. Senbagaraman, A.M. Umarji, Sintering, microstructural and dilatometric studies of combustion synthesized synroc phases, Mater. Res. Bull. 31 (1996) 1375–1381.
[8] S.J. Lee, Y.C. Kim, J.H. Hwang, An organic–inorganic solution technique for fabrication of nano-sized $CaTiO_3$ powder, J. Ceram. Process. Res. 5 (2004) 223–226.
[9] T.R.N. Kutty, R. Vivekanandan, P. Murugaraj, Precipitation of rutile and anatase (TiO_2) fine powders and their conversion to $MTiO_3$ (M = Ba, Sr, Ca) by the hydrothermal method, Mater. Chem. Phys. 19 (1988) 533–546.
[10] A.T. de Figueiredo, V.M. Longo, S. de Lazaro, V.R. Mastelaro, F.S. De Vicente, A.C. Hernandes, M.S. Li, J.A. Varela, E. Longo, Blue-green and red photoluminescence in $CaTiO_3$:Sm, J. Lumin. 126 (2007) 403–407.
[11] A.T. de Figueiredo, S. de Lazaro, E. Longo, E.C. Paris, J.A. Varela, M.R. Joya, P.S. Pizani, Correlation among order–disorder, electronic levels, and photoluminescence in amorphous CT:Sm, Chem. Mater. 18 (2006) 2904–2911.
[12] D. Suvorov, G. Drazic, M. Valant, B. Jancar, Microstructural characterization of $CaTiO_3$–$NdAlO_3$ based ceramics, Korean J. Cryst. 11 (2000) 195–199.
[13] J.S. Kim, C.I. Cheon, H.J. Kang, C.H. Lee, K.Y. Kim, S. Nam, J.D. Byun, Crystal structure and microwave dielectric properties of $CaTiO_3$–$(Li_{1/2}Nd_{1/2})TiO_3$–$(Ln_{1/3}Nd_{1/3})TiO_3$ (Ln = La, Dy) ceramics, Jpn. J. Appl. Phys. 38 (1999) 5633–5637.
[14] D. Suvorov, M. Valant, B. Jancar, S.D. Skapin, $CaTiO_3$-based ceramics: microstructural development and dielectric properties, Acta Chim. Slov. 48 (2001) 87–99.
[15] M. Yoshida, N. Hara, T. Takada, A. Seki, Structure and dielectric properties of $(Ca_{1-x}Nd_{2x/3})TiO_3$, Jpn. J. Appl. Phys. 36 (1997) 6818–6823.
[16] I.S. Kim, W.H. Jung, Y. Inaguma, T. Nakamura, M. Itoh, Dielectric properties of asite deficient perovskite-type lanthanum-calcium-titanium oxide solid solution system $[_{(1-x)}La_{2/3}TiO_{3-x}CaTiO_3$ $(0.1 \le x \le 0.96)]$, Mater. Res. Bull. 30 (1995) 307–316.
[17] W.S. Kim, K.H. Yoon, E.S. Kim, Microwave dielectric properties and far-infrared refractivity characteristics of the $CaTiO_3$–$Li_{1/2-3x}Sm_{1/2+x}TiO_3$ ceramics, J. Am. Ceram. Soc. 83 (2000) 2327–2329.
[18] V.V. Lemanov, A.V. Sotnikov, E.P. Sminova, M. Weihnacht, R. Kunze, Perovskite $CaTiO_3$ as an incipient ferroelectric, Solid State Commun. 110 (1999) 611–614.
[19] Y.X. Wang, W.L. Zhong, C.L. Wang, P.L. Zhang, First-principles study on the tendency to ferroelectricity of $CaTiO_3$, Solid State Commun. 117 (2001) 461–464.
[20] P.T. Diallo, K. Jeanlouis, P. Boutinaud, R. Mahiou, J.C. Cousseins, Improvement of the optical performances of Pr^{3+} in $CaTiO_3$, J. Alloy Compd. 323–324 (2001) 218–222.
[21] P.J. Derén, R. Mahiou, R. Pazika, K. Lemanski, W. Streka, P. Boutinaud, Upconversion emission in $CaTiO_3$:Er^{3+} nanocrystals, J. Lumin. 128 (2008) 797–799.
[22] P.J. Derén, R. Pazik, W. Strek, P. Boutinaud, R. Mahiou, Synthesis and spectroscopic properties of $CaTiO_3$ nanocrystals doped with Pr^{3+} ions, J. Alloy Compd. 451 (2008) 595–599.
[23] E. Pinel, P. Boutinaud, R. Mahiou, What makes the luminescence of Pr^{3+} different in $CaTiO_3$ and $CaZrO_3$? J. Alloy Compd. 380 (2008) 225–229.
[24] P. Boutinaud, E. Pinel, R. Mahiou, Luminescence and afterglow in $CaTiO_3$:Pr^{3+} films deposited by spray pyrolysis, Opt. Mater. 30 (2008) 1033.
[25] W. Sun, S. Zhang, C. Wang, Z. Liu, Z. Mao, Enhanced photocatalytic hydrogen evolution over $CaTi_{1-x}Zr_xO_3$ composites synthesized by polymerized complex method, Catal. Lett. 119 (2007) 148.
[26] E.T. Thostenson, T.W. Chou, Microwave processing: fundamentals and applications, Compos. A: Appl. Sci. Manuf. 30 (1999) 1055–1071.
[27] L.S. Cavalcante, M.F.C. Gurgel, E.C. Paris, A.Z. Simões, M.R. Joya, J.A. Varela, P.S. Pizani, E. Longo, Combined experimental and theoretical investigations of the photoluminescent behavior of $Ba(Ti, Zr)O_3$ thin films, Acta Mater. 55 (2007) 6416–6426.
[28] L.S. Cavalcante, A.Z. Simões, J.C. Sczancoski, V.M. Longo, R. Erlo, M.T. Escote, E. Longo, J.A. Varela, $SrZrO_3$ powders obtained by chemical method: synthesis, characterization and optical absorption behaviour, Solid State Sci. 9 (2007) 1020–1027.
[29] T. Salmi, E. Paatero, P. Nyholm, Kinetic model for the increase of reaction order during polyesterification, Chem. Eng. Proc. 43 (2004) 1487–1493.
[30] D. Keyson, D.P. Volanti, L.S. Cavalcante, A.Z. Simões, I.A. Souza, J.S. Vasconcelos, J.A. Varela, E. Longo, Domestic microwave oven adapted for fast heat treatment of $Ba_{0.5}Sr_{0.5}(Ti_{0.8}Sn_{0.2})O_3$ powders, J. Mater. Process. Technol. 189 (2007) 316–319.
[31] http://icsdweb.fiz-karlsruhe.de/.
[32] T.J.B. Holland, S.A.T. Redfern, Unit cell refinement from powder diffraction data: the use of regression diagnostics, Miner. Mag. 61 (1997) 65–77.
[33] C. Suryanarayana, M.G. Norton, X-Ray Diffraction: A Practical Approach, Plenum Press, New York, 1998.
[34] G. Zhou, M. Lü, F. Gu, D. Xu, D. Yuan, J. Cryst. Growth 276 (2005) 577–582.
[35] H.M. Rietveld, A profile refinement method for nuclear and magnetic structures, J. Appl. Crystallogr. 2 (1969) 65–71.
[36] http://www.ccp14.ac.uk/tutorial/fullprof/index.html.
[37] L.W. Finger, D.E. Cox, A.P. Jephcoat, A correction for powder diffraction peak asymmetry due to axial divergence, J. Appl. Crystallogr. 27 (1994) 892–900.
[38] P.W. Stephens, Phenomenological model of anisotropic peak broadening in powder diffraction, J. Appl. Crystallogr. 32 (1999) 281–289.
[39] U. Balachandran, N.G. Eror, Laser-induced Raman scattering in calcium titanate, Solid State Commun. 44 (1982) 815–818.
[40] S. Qin, X. Wu, F. Seifert, A.I. Becerro, Micro-Raman study of perovskites in the $CaTiO_3$–$SrTiO_3$ system, J. Chem. Soc., Dalton Trans. 19 (2002) 3751–3755.
[41] P. McMillan, N. Ross, Thee Raman-spectra of several orthorhombic calcium-oxide perovskites, Phys. Chem. Miner. 16 (1988) 21–28.
[42] Y. Li, S. Qin, F. Seifert, Phase transitions in A-site substituted perovskite compounds: the $(Ca_{2x}Na_xLa_x)TiO_3$ $(0 \ge x \ge 0.5)$ solid solution, J. Solid State Chem. 180 (2007) 824–833.
[43] T. Hirata, K. Ishioka, M. Kitajima, Vibrational spectroscopy and X-ray diffraction of perovskite compounds $Sr_{1-x}M_xTiO_3$ (M = Ca; Mg; $0 \ge x \ge 1$), J. Solid State Chem. 124 (1996) 353–359.
[44] H. Zheng, G.D.C.C. de Györgyfalva, R. Quimby, H. Bagshaw, R. Ubic, I.M. Reaney, J. Yarwood, Raman spectroscopy of B-site order–disorder in $CaTiO_3$-based microwave ceramics, J. Eur. Ceram. Soc. 23 (2003) 2653–2659.
[45] P. Gillet, F. Guyot, G.D. Price, B. Tournerie, A.L. Cleach, Phase-changes and thermodynamic properties of $CaTiO_3$—spectroscopic data, vibrational modeling and some insights on the properties of $MgSiO_3$ perovskite, Phys. Chem. Miner. 20 (1993) 159–170.
[46] S. Lazaro, J. Milanez, A.T. de Figueiredo, V.M. Longo, V.R. Mastelaro, F.S. De Vicente, A.C. Hernandes, J.A. Varela, E. Longo, Relation between photoluminescence emission and local order–disorder in the $CaTiO_3$ lattice modifier, Appl. Phys. Lett. 90 (2007) 111904–111906.
[47] D.L. Wood, J. Tauc, Weak absorption tails in amorphous semiconductors, Phys. Rev. B 5 (1972) 3144–3151.
[48] Y. Pan, Q. Su, H. Xu, T. Chen, W. Ge, C. Yang, M. Wu, Synthesis and red luminescence of Pr^{3+}-doped $CaTiO_3$ nanophosphor from polymer precursor, J. Solid State Chem. 174 (2003) 69–73.
[49] H. Mizoguchi, K. Ueda, M. Orita, S.-C. Moon, K. Kajihara, M. Hirano, H. Hosono, Decomposition of water by a $CaTiO_3$ photocatalyst under UV light irradiation, Mater. Res. Bull. 37 (2002) 2401–2406.
[50] F.M. Pontes, C.D. Pinheiro, E. Longo, E.R. Leite, S.R. de Lazaro, J.A. Varela, P.S. Pizani, T.M. Boschi, F. Lanciotti, The role of network modifiers in the creation of photoluminescence in $CaTiO_3$, Mater. Chem. Phys. 78 (2002) 227–233.
[51] H.W. Eng, P.W. Barnes, B.M. Auer, P.M. Woodward, Investigations of the electronic structure of d^0 transition metal oxides belonging to the perovskite family, J. Solid State Chem. 175 (2003) 94–109.
[52] L. Grabner, S.E. Stokowski, Photoluminescence of Cr-doped $CaTiO_3$, Phys. Rev. B 2 (1970) 4351–4353.
[53] D.K. Agrawal, Microwave processing of ceramics, Curr. Opin. Solid State Mater. Sci. 3 (1998) 480–485.
[54] K.J. Rao, B. Vaidhyanathan, M. Ganguli, P.A. Ramakrishnan, Synthesis of inorganic solids using microwaves, Chem. Mater. 11 (1999) 882–895.
[55] J. Ma, M. Fang, P. Li, B. Zhu, X. Lu, N.T. Lau, Microwave-assisted catalytic combustion of diesel soot, Appl. Catal. A 159 (1997) 211–228.
[56] W.H. Sutton, W.E. Johnson, United States Patent 4,219,361. Available online at: http://www.freepatentsonline.com/4219361.html.
[57] Y.S. Malghe, A.V. Gurjar, S.R. Dharwadkar, Synthesis of $BaTiO_3$ powder from barium titanyl oxalate (BTO) precursor employing microwave heating technique, Bull. Mater. Sci. 27 (2004) 217–220.
[58] B.M. Patil, R.S. Srinivasa, S.R. Dharwadkar, Synthesis of $CaTiO_3$ from calcium titanyl oxalate hexahydrate (CTO) as precursor employing microwave heating technique, Bull. Mater. Sci. 30 (2007) 225–229.
[59] A.Z. Simões, C.S. Riccardi, M.A. Ramírez, L.S. Cavalcante, E. Longo, J.A. Varela, Synthesis and characterization of $CaBi_4Ti_4O_{15}$ thin films annealed by microwave and conventional furnaces, Solid State Sci. 9 (2007) 756–760.